Transition between localized and extended states in the hierarchical Anderson model

F. L. Metz,[1] L. Leuzzi,[1,2] G. Parisi,[1,2,3] and V. Sacksteder IV[4]

[1]*Dipartimento di Fisica, Università La Sapienza, Piazzale A. Moro 2, I-00185, Rome, Italy*

[2]*IPCF-CNR, UOS Roma Kerberos, Università La Sapienza, P. le A. Moro 2, I-00185, Rome, Italy*

[3]*INFN, Piazzale A. Moro 2, 00185, Rome, Italy*

[4]*Institute of Physics, Chinese Academy of Sciences, Beijing 100190, China*

(Received 14 March 2013; revised manuscript received 13 April 2013; published 2 July 2013)

We present strong numerical evidence for the existence of a localization-delocalization transition in the eigenstates of the 1D Anderson model with long-range hierarchical hopping. Hierarchical models are important because of the well-known mapping between their phases and those of models with short-range hopping in higher dimensions, and also because the renormalization group can be applied exactly without the approximations that generally are required in other models. In the hierarchical Anderson model, we find a finite critical disorder strength W_c where the average inverse participation ratio goes to zero; at small disorder, $W < W_c$, the model lies in a delocalized phase. This result is based on numerical calculation of the inverse participation ratio in the infinite volume limit using an exact renormalization group approach facilitated by the model's hierarchical structure. Our results are consistent with the presence of an Anderson transition in short-range models with $D > 2$ dimensions, which was predicted using renormalization group arguments. Our finding should stimulate interest in the hierarchical Anderson model as a simplified and tractable model of the Anderson localization transition, which occurs in finite-dimensional systems with short-range hopping.

DOI: 10.1103/PhysRevB.88.045103 PACS number(s): 71.23.An, 05.10.Cc

I. INTRODUCTION

After more than fifty years, the Anderson transition[1] between localized and extended wave functions of a single quantum particle moving in a disordered medium remains the focus of considerable interest.[2,3] Crucial contributions to this field have been made by exactly solvable tight-binding models, such as 1D models with nearest-neighbour hopping[2,4] and models on the Bethe lattice.[5,6] Here, we consider another interesting class of tight-binding models with long-range hopping arranged in a hierarchical block structure and decaying according to a power law with exponent α. Hierarchical models have a long history in statistical physics starting with Dyson,[7] and (as we will explain later) they provide an indirect route to understanding phases and critical behavior in D-dimensional systems.[8]

We study the hierarchical Anderson model (HAM) introduced by Bovier, which combines on-site disorder with hierarchically structured long-range hopping.[9] In the absence of disorder, the spectrum is an infinite set of highly degenerate flat bands that accumulate at the upper spectral edge. The degeneracies are arranged in a geometric series: one-half of the pure HAM's states lie in the lowest energy band, one quarter in the next highest energy, etc. Hierarchical models preserve their structure under renormalization group transformations,[9–11] which has allowed proof of several rigorous results about the site disordered HAM's spectrum,[8,12–15] and may promise exact extensions of the successful scaling theory of localization.[16] In particular, the absolutely continuous part of the spectrum vanishes and the model presents only spectral localization, provided that the hopping decays sufficiently quickly with distance, i.e., the hopping decay exponent $\alpha > 3/2$.[12,13]

Unfortunately, much less is known about the size of the HAM's eigenvectors. The degeneracies of the pure model permit different choices of mutually orthogonal sets of eigenvectors. The most extended set consists of infinitely extended plane waves, while the least extended set has sizes that are strongly band dependent, with very localized states in the lowest band and infinitely extended states in the highest band. In the presence of on-site disorder, it recently has been argued that all states are always localized,[17] based on an analogy with the criticality results for random-matrix models, such as ensembles of ultrametric[18,19] and power-law random banded matrices.[20] Both models, characterized by an exponent α controlling the power-law decaying *random* hoppings, exhibit an extended phase for $\alpha < 1$ and a localized phase for $\alpha > 1$. This would rule out the possibility of a transition in the HAM, which has a well-defined macroscopic limit only for $\alpha > 1$. However, models with random hopping are relatively simple: the scattering length vanishes and only the localization length is important. The HAM belongs instead to the class of models with *deterministic* hopping, which are much richer because they have nontrivial physics at both length scales. In particular, the 1D Anderson model with on-site disorder and deterministic power-law hopping exhibits a localization transition at its upper spectral edge.[21–25]

In this work, we show that the HAM exhibits a localization-delocalization transition near its upper spectral edge. We perform a thorough numerical study of the inverse participation ratio, which is the inverse of the eigenstate volume. Thanks to the HAM's invariance under block renormalization group (RG) transformations, we obtain recurrence equations for calculating the resolvent matrix. This recursive method allows us to calculate the IPR in systems large enough to precisely determine their infinite size behavior. Our results also suggest that there is a critical value of α above which all states are localized, in analogy with the lower critical dimension $D = 2$ below which finite-dimensional short-range systems are always localized and above which an Anderson transition was predicted using RG arguments.[16]

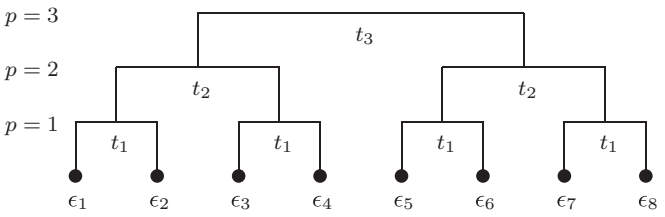

FIG. 1. Schematic representation of the hierarchical Anderson model, cf. Eq. (1), with $L = 2^3$ sites. Lines denote hopping energies t_p between sites in distinct blocks of size 2^{p-1}.

II. THE HIERARCHICAL ANDERSON MODEL.

The HAM is a 1D tight-binding model with $L = 2^N$ equally spaced sites and independently distributed random site potentials ϵ_i, $i = 1, \ldots, L$, with zero mean and standard deviation W. The Hamiltonian reads

$$\mathcal{H}_N = \sum_{i=1}^{2^N} \epsilon_i |i\rangle\langle i| + \sum_{p=1}^{N} V_p \sum_{r=1}^{2^{N-p}} \sum_{i\neq j}^{1,2^p} |(r-1)2^p + i\rangle\langle(r-1)2^p + j|, \quad (1)$$

where $|i\rangle$ is the canonical site basis. The second line is the hierarchical hopping matrix introduced by Dyson.[7] It is the heart of the hierarchical Anderson model, and is organized in a tree as illustrated in Fig. 1. The highest level of the tree has index $p = N$ and the lowest level has index $p = 1$. At each level, the system is divided into 2^{N-p} separate blocks, each of which contains 2^p sites. The hopping between any two sites within a single block has energy V_p. As seen in Fig. 1, the hopping between sites in two different blocks is determined by levels higher in the hierarchy and has energy $t_p = \sum_{n=p}^{N} V_n$. We study the deterministic HAM, which has hopping energies $V_p = 2^{-\alpha(p-1)}$. This exponential decay in the level index p ensures that in large $N \gg 1$ systems the hopping energy between sites separated by a distance $O(L)$ decays according to a power law $t_p \propto O(L^{-\alpha})$, the same as 1-D Anderson models with power-law hopping.[21–25]

We study the infinite volume limit of the average density of states (DOS) $\rho(E)$ and of the inverse participation ratio $P(E)$. The former is defined as

$$\rho(E) = \lim_{L\to\infty} \left\langle \frac{1}{L} \sum_{\mu=1}^{L} \delta(E - E_\mu) \right\rangle, \quad (2)$$

where $\langle \cdots \rangle$ is the average with respect to the disorder potential ϵ_i and E_μ are the HAM's eigenvalues. The DOS measures the averaged spectrum, but does not contain any signal of the eigenstates' localization or delocalization. We therefore study the average inverse participation ratio (IPR) of the normalized eigenstates $|\psi_\mu\rangle$:[26–28]

$$P(E) = \lim_{L\to\infty} \frac{1}{L\rho(E)} \left\langle \sum_{\mu=1}^{L} I_\mu^L \delta(E - E_\mu) \right\rangle, \quad (3)$$

where $I_\mu^L = \sum_{i=1}^{L} (\langle i|\psi_\mu\rangle)^4$ is the IPR of an individual eigenstate. Its inverse measures the eigenstate's volume. The IPR is restricted to the interval $0 \leqslant P(E) \leqslant 1$. States that are perfectly localized on a single site satisfy $P(E) = 1$, and states that are equally distributed across all sites satisfy $P(E) = 1/L \to 0$.

In the pure ordered HAM ($W = 0$), the DOS is a series of flat bands $\rho_{\text{pure}}(E) = \sum_{p=1}^{\infty} 2^{-p} \delta(E - E_{p-1}^{\text{pure}})$. Each flat band is related to a level in the HAM's hierarchy. The bands' degeneracy decreases repeatedly by factors of two as one moves to higher energy, thus yielding the factor 2^{-p}. The difference between consecutive energetic levels falls off as $E_{p+1}^{\text{pure}} - E_p^{\text{pure}} \propto 2^{-(\alpha-1)p}$ and, hence, these accumulate at the upper spectral edge E_∞^{pure}. Near E_∞^{pure} the integrated density of states $\mathcal{N}(E_p^{\text{pure}}) = \sum_{\ell=1}^{p} 2^{-\ell}$ follows a power law similar to that of short-range finite-dimensional systems: $\mathcal{N}(E_p^{\text{pure}}) = 1 - C(E_\infty^{\text{pure}} - E_p^{\text{pure}})^{d_s/2}$.[8,12,14,15] Here, $d_s = 2/(\alpha - 1)$ is the *spectral dimension* which controls both diffusion and the long-distance physics of second-order phase transitions such as the Anderson transition. For $W > 0$, the integrated DOS of the HAM exhibits a Lifshitz tail at the upper spectral edge, with a Lifshitz exponent given by the spectral dimension.[15] This is the same behavior as observed in short-range finite-dimensional systems with on-site disorder, where the integrated DOS exhibits a Lifshitz tail controlled by the Euclidean dimension.[29] Overall, as E_∞^{pure} is approached, the spectral properties of the pure HAM become similar to short-range finite-dimensional systems. This is, thus, the most promising region for studying localization transitions. Much of the interest in hierarchical models originates in their mapping to short-range models whose Euclidean dimension is strictly related to the spectral dimension (see, e.g., Ref. 30 and references therein).

III. RENORMALIZATION EQUATIONS FOR THE RESOLVENT

We obtain the DOS and IPR from the diagonal elements of the resolvent matrix $\boldsymbol{G}^{(N)}(z) = (z - \mathcal{H}_N)^{-1}$, where $z = E - i\eta$, and η is a small positive regularizer that smooths our numerical results over an interval in the spectrum with width proportional to η.[31,32] We use the following formulas:[26,27,33,34]

$$\rho(E) = \lim_{\eta\to 0^+} \lim_{L\to\infty} \frac{1}{L\pi} \sum_{i=1}^{L} \left\langle \text{Im}\, G_i^{(N)}(z) \right\rangle, \quad (4)$$

$$P(E) = \lim_{\eta\to 0^+} \lim_{L\to\infty} \frac{\eta}{\pi L\rho(E)} \sum_{i=1}^{L} \left\langle \left| G_i^{(N)}(z) \right|^2 \right\rangle. \quad (5)$$

The HAM's hierarchical structure allowed us to develop a block RG approach which recursively calculates the resolvent for one instance of the disorder. Our calculation has two phases: a sweep up the hierarchy, and then a sweep back down. At each step ℓ of the sweep up we remove the basis states associated with one flat band, and calculate an energy-dependent effective Hamiltonian, which acts in the reduced basis but exhibits the same poles found in the original full-basis Hamiltonian. This effective Hamiltonian retains the hierarchical form but its hopping energies $\{V_p^{(\ell)}\}$ and disorder

potentials $\{\mu_i^{(\ell)}\}$ are renormalized according to

$$\mu_i^{(\ell)} = \frac{2\mu_{2i-1}^{(\ell-1)}\mu_{2i}^{(\ell-1)}}{\mu_{2i-1}^{(\ell-1)} + \mu_{2i}^{(\ell-1)}} + 2V_1^{(\ell-1)}, \quad i = 1, \ldots, 2^{N-\ell}, \tag{6}$$

$$V_p^{(\ell)} = 2V_{p+1}^{(\ell-1)}, \quad p = 1, \ldots, N-\ell\,. \tag{7}$$

Hopping energies and disorder potentials at the beginning of the sweep up, $V_p^{(0)} = V_p$ and $\mu_i^{(0)} = \epsilon_i - z - \sum_{p=1}^{N} V_p$, are those of the original hierarchical Hamiltonian. After $\ell = N$ steps we reach the top of the hierarchy and obtain a single site effective Hamiltonian with disorder potential $\mu_1^{(N)}$. The resolvent of this Hamiltonian is simply $G_1^0(z) = -1/\mu_1^{(N)}$. We use this resolvent to begin the sweep back down in which we progressively restore the original basis and recursively calculate the resolvent's diagonal elements in the restored basis:

$$G_{2i-1}^{(N-\ell+1)}(z) = 2\left[\frac{\mu_{2i}^{(\ell-1)}}{\gamma_i^{(\ell-1)}}\right]^2 G_i^{(N-\ell)}(z) - \frac{1}{\gamma_i^{(\ell-1)}}, \tag{8}$$

$$G_{2i}^{(N-\ell+1)}(z) = 2\left[\frac{\mu_{2i-1}^{(\ell-1)}}{\gamma_i^{(\ell-1)}}\right]^2 G_i^{(N-\ell)}(z) - \frac{1}{\gamma_i^{(\ell-1)}}, \tag{9}$$

with $\gamma_i^{(\ell-1)} = \mu_{2i-1}^{(\ell-1)} + \mu_{2i}^{(\ell-1)}$. This procedure yields the diagonal elements of the resolvent in the original system, and its memory consumption and computational time grow only linearly with L.[40] The derivation of Eqs. (6)–(9) is presented in Appendix A.

IV. RESULTS

Figure 2 compares the DOS and IPR calculated with our renormalization method (solid lines) and $\eta = 0.005$ to standard numerical diagonalization (filled circles) in a system of size $L = 2^{10}$. The potential ϵ_i is generated from a Gaussian distribution with zero mean and standard deviation W. Diagonalization results are averaged over $\mathcal{N}_\epsilon = 10^3$ disorder realizations and renormalization results over $\mathcal{N}_\epsilon = 2 \times 10^4$ realizations. Figure 2 shows excellent agreement between the two methods.

The only important discrepancy is found in the IPR at small disorder $W = 0.6$, where the DOS falls precipitously. The observed discrepancy is explained by Fig. 2 inset, which compares results with two values of the regularization parameter: $\eta = 0.01$ and 0.005. The latter lies closer to the diagonalization results, which indicates that when the disorder is small the limit $\eta \to 0^+$ is reached only at $\eta \ll 0.005$.

Figure 2 also gives an overview of the DOS and IPR across the spectrum for a representative hopping decay exponent $\alpha = 7/4$ and four different values of the disorder strength $W = 0.6, 1.0, 1.4, 1.8$. At small disorder $W = 0.6$, the average DOS is separated into several bands whose positions coincide with the pure system's flat bands. The associated minima in $P(E)$ show that the eigenstates are bigger in the band centers and smaller at the band edges. When the disorder is increased, the bands progressively blur together and $P(E)$ steadily increases as the eigenstates become ever more localized. Figure 3 shows the same behavior at $\alpha = 3/2$ in systems of size $L = 2^{23}$. Reaching such large sizes allows us to explore smaller η values and obtain detailed results about many bands near the upper

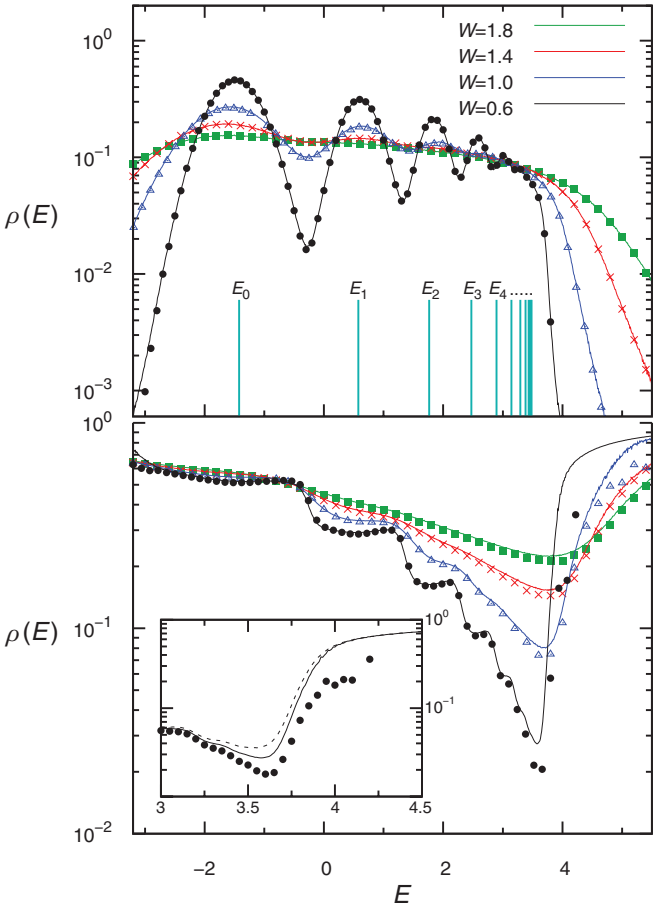

FIG. 2. (Color online) Comparison of the HAM's average DOS and IPR: numerical diagonalization (filled circles) vs RG method (solid lines), with hopping decay exponent $\alpha = 7/4$. The energies of the pure model's flat bands are marked with cyan vertical lines in the upper pane. The inset shows that when the IPR is small the RG method is sensitive to the spectral line width η; the dashed and solid lines were obtained with $\eta = 0.01$ and 0.005, respectively.

spectral edge. Indeed, in order to obtain statistically significant results, the spectral line width η must considerably exceed the mean level spacing $[N\rho(E)]^{-1}$.

In general, the IPR exhibits several local minima corresponding to large states near the centers of the HAM's bands, and the global minimum lies near HAM's upper spectral edge. In order to verify the existence of extended states at finite W we focus on the asymptotic value of the global minimum of the IPR, $P_{\min}(W)$, in the $L \to \infty$ limit and for infinitesimal $\eta \to 0^+$. The main graph in Fig. 4 summarizes our calculation of $P_{\min}(W)$ for a particular hopping decay $\alpha = 3/2$ and disorder strength $W = 0.8$, which lie close to the delocalization transition. We display the IPR of a very large $L = 2^{27}$ system at three different values of η. Statistical errors at smaller η are larger because of η's proximity to the level spacing. Appendix B includes a detailed discussion of these errors in the limit $\eta \to 0^+$. In particular, we have checked that for $L \geqslant 2^{26}$ the IPR curves at fixed η do not change with L, which signals that they accurately represent the infinite volume limit.

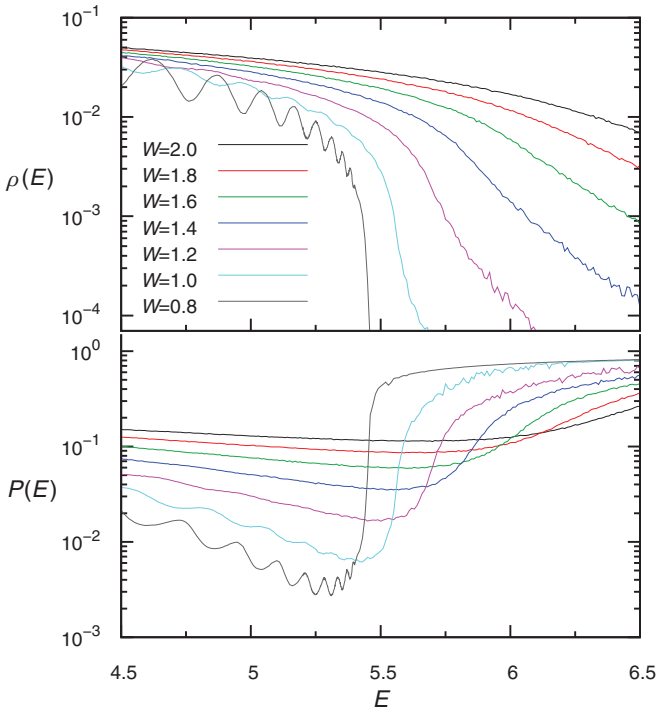

FIG. 3. (Color online) Average DOS and IPR near the upper spectral edge in a large $L = 2^{23}$ system at several disorder strengths and $\alpha = 3/2$, $\eta = 5 \times 10^{-4}$, and $\mathcal{N}_\epsilon = 30$.

The IPR depends on η, and as $\eta \to 0^+$ the global minimum deepens and shifts toward higher energy. This effect is not significant at larger disorder $W > 1.0$, but at smaller disorder it forces us to use considerable care with the $\eta \to 0^+$ extrapolation. The inset in Fig. 4 displays our extrapolation to the limit $\eta \to 0^+$ at four weak disorder strengths. At each W, we find the energy $E_{\min}(W)$ of the local minimum at

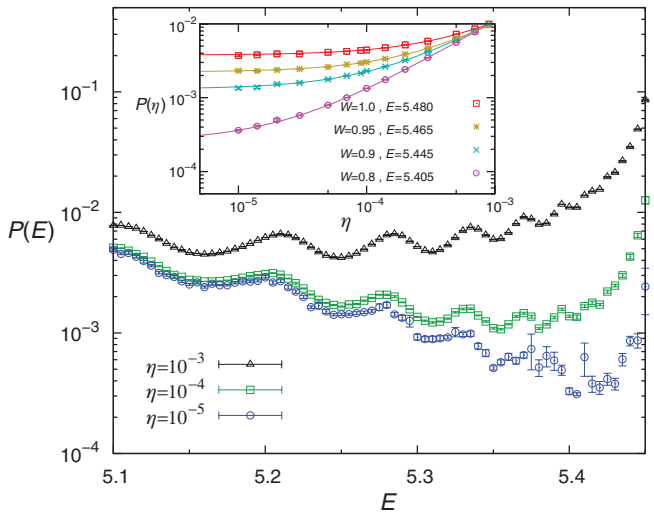

FIG. 4. (Color online) The $\eta \to 0^+$ limit. The three curves show the average IPR at three values of η and $\alpha = 3/2$, $W = 0.8$, $L = 2^{27}$, and $\mathcal{N}_\epsilon = 10$. The global minimum decreases and shifts to higher energy. The inset shows the IPR versus η at the energy of the global minimum. Again $\alpha = 3/2$, but now $L = 2^{28}$ and $\mathcal{N}_\epsilon = 100$. The solid lines are linear fits to $P(\eta) = P_{\min} + b\eta$.

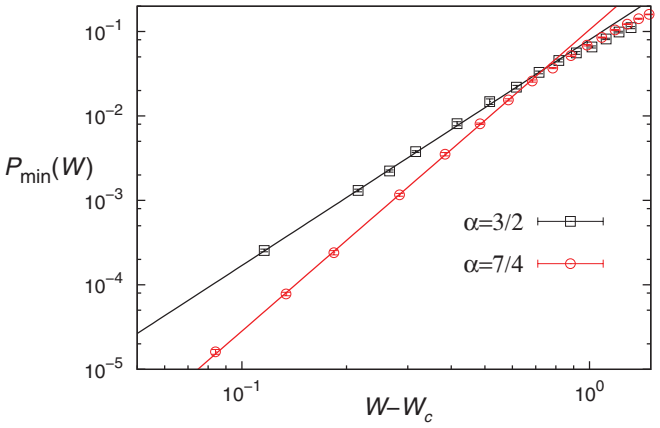

FIG. 5. (Color online) Power law behavior of the minimum IPR $P_{\min}(W)$ near the critical disorder strength W_c where it converges to zero. Solid lines represent the power-law fit $P_{\min}(W) = A(W - W_c)^{\pi_2}$, with parameters from Table I.

the lowest value of the spectral width parameter employed, $\eta = 10^{-5}$, and then graph the IPR at that energy as a function of η. Concerning uncertainty in $E_{\min}(W)$, we have checked that it affects our results only slightly, and in any case can only cause an unduly careful overestimate of the IPR. The fitting curves in Fig. 4 show that the IPR depends linearly on η via $P(\eta) = P_{\min} + b\eta$. This allows us to determine very accurately the asymptotic global minimum of the IPR.

The straight lines in Fig. 5's log-log plot are the central result of our work: strong numerical evidence that the minimum IPR $P_{\min}(W)$ converges to zero according to a power law $P_{\min}(W) = A(W - W_c)^{\pi_2}$, similar to the power law observed in finite-dimensional short-range systems.[26,35,36] At smaller disorder $W \leqslant W_c$, the HAM exhibits a delocalized phase. Table I reports the best fit parameters for two values of the hopping decay exponent $\alpha = 3/2, 7/4$. In both cases, our data exclude the possibility that $W_c = 0$.

V. CONCLUSIONS.

We have analyzed the DOS and the IPR of the hierarchical Anderson model by means of a RG-based calculation of the resolvent matrix, finding strong evidence for a localization-delocalization transition at finite disorder at $\alpha = 3/2$ and $7/4$. Since it has been proven rigorously that the absolutely continuous part of the spectrum vanishes for $\alpha > 3/2$,[12] our results indicate that spectral localization may not imply the existence of exponentially localized eigenvectors. A study of the spatial decay of the resolvent elements should clarify this point and we expect our work to stimulate further research in this direction. Our results also indicate that the HAM differs

TABLE I. Values of the parameters and the χ^2 of the power law fit to the IPR data shown in Fig. 5. W_c is the critical disorder where the delocalization transition occurs and π_2 is a critical exponent.

α	W_c	π_2	A	χ^2/ndf	ndf
3/2	0.684(7)	2.68(7)	0.080(2)	0.96	6
7/4	0.016(5)	3.57(8)	0.105(3)	1.21	5

from the 1D tight-binding model with power-law hopping,[23,24] where all states are localized for $\alpha \geqslant 3/2$.[24] Since the HAM's spectral dimension can be mapped to the spatial dimension of Anderson models with short-range hopping, we expect that an Anderson transition exists in the regime $1 < \alpha < 2$, with $\alpha \simeq 2$ playing a role analogous to the lower critical dimension. The presence of extended states in one dimension is not exclusive to models with long-range hopping, but it has been also observed in systems with short-range hopping and correlated on-site disorder.[37–39] Lastly, we mention that our RG method can be used to compute off-diagonal elements of the resolvent, allowing determination of other relevant quantities such as the longest localization length.[2,4]

ACKNOWLEDGMENTS

F.L.M. is greatly indebted to Lucas Nicolao, Jacopo Rocchi, Pierfrancesco Urbani, and Izaak Neri for many interesting and useful discussions. V.S. thanks Tomi Ohtsuki and Koji Kobayashi for discussions and hospitality. The research leading to these results has received funding from the European Research Council (ERC) grant agreement No. 247328 (CriPheRaSy project), from the People Programme (Marie Curie Actions) of the European Union's Seventh Framework Programme FP7/2007-2013/ under REA grant agreement No. 290038 (NETADIS project), and from the Italian MIUR under the Basic Research Investigation Fund FIRB2008 program, grant No. RBFR08M3P4, and under the PRIN2010 program, grant code 2010HXAW77-008.

APPENDIX A: DERIVATION OF THE RENORMALIZATION EQUATIONS

We discuss here how to derive the RG equations (6)–(9) that are used in the main text. This calculation can be performed using only linear algebra, but we find it more convenient to use Gaussian integrals. We first rewrite $\{G_k^{(N)}(z)\}_{k=1,\ldots,L}$, the diagonal elements of the resolvent $\boldsymbol{G}^{(N)}(z) = (z - \mathcal{H}_N)^{-1}$, as the Gaussian integrals

$$G_k^{(N)}(z) = \imath \frac{\int d\boldsymbol{\phi}\, \phi_k^2 \exp[\mathcal{L}^{(N)}(\phi_{1,\ldots,2^N})]}{\int d\boldsymbol{\phi} \exp[\mathcal{L}^{(N)}(\phi_{1,\ldots,2^N})]},$$
$$\mathcal{L}^{(N)}(\phi_{1,\ldots,2^N}) = \frac{\imath}{2}\sum_{j=1}^{2^N} \mu_j \phi_j^2 + W^{(N)}(\phi_{1,\ldots,2^N}; V_{1,\ldots,N}), \tag{A1}$$

where $d\boldsymbol{\phi} = \prod_{j=1}^{2^N} d\phi_j$ and $\mu_j = \epsilon_j - z - \sum_{p=1}^{N} V_p$. The function $W^{(N)}$ encodes the hierarchical hoppings:

$$W^{(N)}(\phi_{1,\ldots,2^N}; V_{1,\ldots,N}) = \frac{\imath}{2}\sum_{p=1}^{N} V_p \sum_{r=1}^{2^{N-p}} \left[\sum_{j=1}^{2^p} \phi_{(r-1)2^p+j}\right]^2.$$

We have introduced the simplified notation $x_{1,\ldots,\mathcal{A}} \equiv x_1, \ldots, x_{\mathcal{A}}$. The function $\mathcal{L}^{(N)}(\phi_{1,\ldots,2^N})$ has the same form as the HAM's Hamiltonian and therefore preserves its formal structure under a RG transformation: a local term incorporating the random potential and a nonlocal hierarchical hopping term. We make a change of integration variables

$$\psi_j^{\pm} = \frac{1}{\sqrt{2}}(\phi_{2j-1} \pm \phi_{2j}), \quad j = 1, \ldots, 2^{N-1},$$

which transforms the hierarchical term as follows:

$$W^{(N)}(\phi_{1,\ldots,2^N}; V_{1,\ldots,N}) = \imath V_1 \sum_{j=1}^{2^{N-1}} (\psi_j^+)^2 + W^{(N-1)}(\psi^+_{1,\ldots,2^{N-1}}; V'_{1,\ldots,N-1}),$$

where $V'_p = 2V_p$. This transformation allows us to explicitly calculate the integrals over $\{\psi_j^-\}_{j=1,\ldots,2^{N-1}}$ in Eq. (A1), halving the number of degrees of freedom. After performing the transformation and integration we obtain an equation which relates $\{G_i^{(N)}(z)\}_{i=1,\ldots,L}$ for the original model with L sites to $\{G_i^{(N-1)}(z)\}_{i=1,\ldots,L/2}$ for a model with $L/2$ sites, but with renormalized parameters.

Partitioning $\{G_i^{(N)}(z)\}_{i=1,\ldots,2^N}$ into two sectors (one for the even sites and another for the odd sites), we obtain the following expressions:

$$G_{2k-1}^{(N)}(z) = \frac{\imath}{2}\frac{\int d\boldsymbol{\psi}^+ d\boldsymbol{\psi}^- (\psi_k^+ + \psi_k^-)^2 e^{H^{(N-1)}(\psi^{\pm})}}{\int d\boldsymbol{\psi}^+ d\boldsymbol{\psi}^- e^{H^{(N-1)}(\psi^{\pm})}}, \tag{A2}$$

$$G_{2k}^{(N)}(z) = \frac{\imath}{2}\frac{\int d\boldsymbol{\psi}^+ d\boldsymbol{\psi}^- (\psi_k^+ - \psi_k^-)^2 e^{H^{(N-1)}(\psi^{\pm})}}{\int d\boldsymbol{\psi}^+ d\boldsymbol{\psi}^- e^{H^{(N-1)}(\psi^{\pm})}}. \tag{A3}$$

In the above expressions, we have changed integration variables to $d\boldsymbol{\psi}^{\pm} = \prod_{j=1}^{2^{N-1}} d\psi_j^{\pm}$ and we have defined

$$H^{(N-1)}(\psi^{\pm}) = \frac{\imath}{2}\sum_{j=1}^{2^{N-1}} \sigma_j (\psi_j^+)^2 + \frac{\imath}{2}\sum_{j=1}^{2^{N-1}} \Delta_j (\psi_j^-)^2 + \imath \sum_{j=1}^{2^{N-1}} C_j \psi_j^+ \psi_j^- + W^{(N-1)}(\psi^+_{1,\ldots,2^{N-1}}; V'_{1,\ldots,N-1}),$$

where the following quantities are complex valued:

$$\sigma_j = \tfrac{1}{2}(\mu_{2j-1} + \mu_{2j}) + 2V_1,$$
$$\Delta_j = \tfrac{1}{2}(\mu_{2j-1} + \mu_{2j}),$$
$$C_j = \tfrac{1}{2}(\mu_{2j-1} - \mu_{2j}).$$

Since Eqs. (A2) and (A3) involve only simple Gaussian integrals with respect to $\psi^-_{1,\ldots,2^{N-1}}$, these variables can be integrated out one by one. We map the resulting expression to Eq. (A1) for a system with 2^{N-1} sites, renormalized disorder $\mu'_{1,\ldots,2^{N-1}}$, which obeys Eq. (8) in the main text, and renormalized hopping potential $V'_{1,\ldots,N-1}$. We obtain Eqs. (6)–(9) at the first RG step $\ell = 1$ of the original model. Performing these steps recursively leads to the recurrence equations (6) and (7) shown in the main text:

$$G_{2i-1}^{(N-\ell+1)}(z) = 2\left[\frac{\mu_{2i}^{(\ell-1)}}{\gamma_i^{(\ell-1)}}\right]^2 G_i^{(N-\ell)}(z) - \frac{1}{\gamma_i^{(\ell-1)}},$$
$$G_{2i}^{(N-\ell+1)}(z) = 2\left[\frac{\mu_{2i-1}^{(\ell-1)}}{\gamma_i^{(\ell-1)}}\right]^2 G_i^{(N-\ell)}(z) - \frac{1}{\gamma_i^{(\ell-1)}},$$

where $\gamma_i^{(\ell)} = \mu_{2i-1}^{(\ell)} + \mu_{2i}^{(\ell)}$.

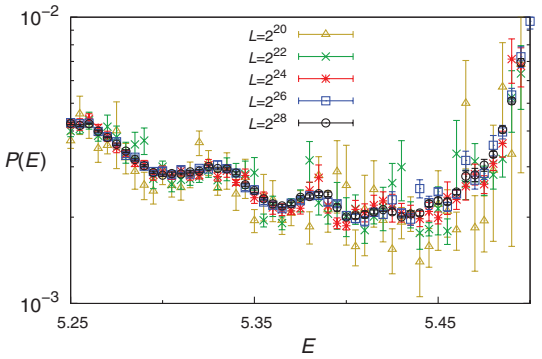

FIG. 6. (Color online) Size effects on the IPR at $\alpha = 1.5$, $W = 0.9$, $\eta = 10^{-4}$, and $\mathcal{N}_\epsilon = 10$.

APPENDIX B: PERFORMING THE $\eta \to 0^+$ LIMIT NUMERICALLY

The regularization parameter η in the resolvent gives each eigenvalue a line width proportional to η. This can be understood by analyzing our equation for the DOS:

$$\rho(E) = \lim_{\eta\to 0^+} \lim_{L\to\infty} \frac{1}{L\pi} \sum_{i=1}^{L} \left|\mathrm{Im}\, G_i^{(N)}(z)\right|. \tag{B1}$$

The right-hand side of this equation is the limit $\eta \to 0^+$ of a sum of Lorentzian functions with width η and centered at E. The Lorentzians quantify the distances of $\mathcal{H}_N$'s eigenvalues from the energy E. As η approaches the mean level spacing from above, our observables will display larger and larger fluctuations, since our averages will include smaller and smaller numbers of eigenstates. If η is smaller than the level spacing then one obtains results that have no physical meaning. Accurate results for very small η are obtained only if the system size L and the number of samples $\mathcal{N}_\epsilon$ are large enough. Figure 6 shows how this issue influences the IPR. We fix the number of samples $\mathcal{N}_\epsilon$ and spectral line width η and vary the system size. Convergence is obtained at $L \geqslant 2^{26}$.

If we define $\rho_{L,\mathcal{N},\eta}(E)$ as the average DOS of a finite though very large system, we can estimate the mean level spacing $\Delta_{L,\mathcal{N},\eta}(E)$ around E as

$$\Delta_{L,\mathcal{N},\eta}(E) \sim \frac{1}{L\mathcal{N}_\epsilon \rho_{L,\mathcal{N},\eta}(E)}.$$

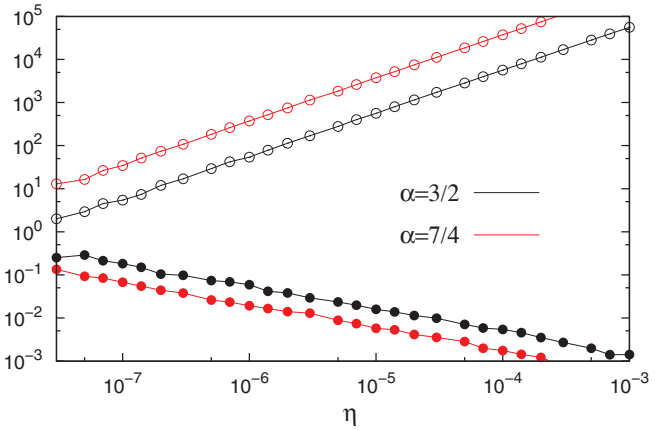

FIG. 7. (Color online) η dependence of the ratios $\eta/\Delta_{L,\mathcal{N},\eta}(E)$ (open circles) and $\sigma_{L,\mathcal{N},\eta}(E)/\rho_{L,\mathcal{N},\eta}(E)$ (filled circles). $\Delta_{L,\mathcal{N},\eta}(E)$ is the approximate mean level spacing and $\sigma_{L,\mathcal{N},\eta}(E)$ is the standard deviation around $\rho_{L,\mathcal{N},\eta}(E)$. Results were obtained using Eqs. (6)–(9) in the main text with $N = 28$ and $\mathcal{N}_\epsilon = 100$. We set $(W = 0.8, E = 5.405)$ for $\alpha = 3/2$ and $(W = 0.2, E = 3.532)$ for $\alpha = 7/4$. These values were used to produce the left-most (smallest disorder) data point in Fig. 5 of the main text.

We estimate the error at small η by calculating $\sigma_{L,\mathcal{N},\eta}(E)/\rho_{L,\mathcal{N},\eta}(E)$ and $\eta/\Delta_{L,\mathcal{N},\eta}$, where $\sigma_{L,\mathcal{N},\eta}(E)$ is the standard deviation of $\rho_{L,\mathcal{N},\eta}(E)$. Typical results are displayed in Fig. 7. When we decrease $\eta \to 0^+$ we find monotonic growth in $\sigma_{L,\mathcal{N},\eta}(E)/\rho_{L,\mathcal{N},\eta}(E)$ and monotonic decay in $\eta/\Delta_{L,\mathcal{N},\eta}$. For small enough η, we reach a regime where $\sigma_{L,\mathcal{N},\eta}(E)/\rho_{L,\mathcal{N},\eta}(E) = O(1)$, $\eta/\Delta_{L,\mathcal{N},\eta} = O(1)$, and $\rho_{L,\mathcal{N},\eta}(E)$ exhibits large fluctuations. We conclude that the limit $\eta \to 0^+$ is achieved, for practical purposes, when $\Delta_{L,\mathcal{N},\eta} \ll \eta \ll 1$, i.e., in very large systems. Therefore we establish a sensible lower cutoff on η by imposing a maximum value of the average DOS's relative error $\sigma_{L,\mathcal{N},\eta}(E)/\rho_{L,\mathcal{N},\eta}(E)$.

The results for the minimum IPR displayed in Fig. 5 of the main text were obtained by choosing $\eta = 10^{-5}$ as the lower cutoff when $\alpha = 3/2$ and $\eta \in [10^{-7}, 10^{-5}]$ when $\alpha = 7/4$. This ensures that the relative error $\sigma_{L,\mathcal{N},\eta}(E)/\rho_{L,\mathcal{N},\eta}(E)$ is restricted to the interval $[10^{-2}, 10^{-1}]$, as can be seen in Fig. 7.

[1] P. W. Anderson, Phys. Rev. **109**, 1492 (1958).
[2] B. Kramer and A. MacKinnon, Rep. Prog. Phys. **56**, 1469 (1993).
[3] F. Evers and A. D. Mirlin, Rev. Mod. Phys. **80**, 1355 (2008).
[4] E. N. Economou, *Green's Functions in Quantum Physics* (Springer, Heidelberg, 2006).
[5] R. Abou-Chacra, P. W. Anderson, and D. J. Thouless, J. Phys. C: Solid State Phys. **6**, 1734 (1973).
[6] R. Abou-Chacra and D. J. Thouless, J. Phys. C: Solid State Phys. **7**, 65 (1974).
[7] F. J. Dyson, Commun. Math. Phys. **12**, 91 (1969).
[8] S. Molchanov, in *Proceedings of the Sixth Eugene Lucaks Symposium*, edited by A. K. Gupta and V. L. Girko (VSP, Utrecht, The Netherlands, 1996), pp. 179–194.
[9] A. Bovier, J. Stat. Phys. **59**, 745 (1990).
[10] G. Baker, Phys. Rev. B **5**, 2622 (1972).
[11] Y. Meurice, J. Phys. A: Math. Theor. **40**, R39 (2007).
[12] E. Kritchevski, Proc. Am. Math. Soc. **135**, 1431 (2007).
[13] E. Kritchevski, in *CRM Proceedings and Lectures Notes*, Vol. 42 (American Mathematical Society, Providence, USA, 2007).
[14] E. Kritchevski, Ann. Henri Poincare **9**, 685 (2008).
[15] S. Kuttruf and P. Möller, Ann. Henri Poincare **13**, 525 (2012).
[16] E. Abrahams, P. W. Anderson, D. C. Licciardello, and T. V. Ramakrishnan, Phys. Rev. Lett. **42**, 673 (1979).
[17] C. Monthus and T. Garel, J. Stat. Mech. (2011) P05005.
[18] Y. V. Fyodorov, A. Ossipov, and A. Rodriguez, J. Stat. Mech. (2009) L12001.

[19]E. Bogomolny and O. Giraud, Phys. Rev. Lett. **106**, 044101 (2011).
[20]A. D. Mirlin, Y. V. Fyodorov, F.-M. Dittes, J. Quezada, and T. H. Seligman, Phys. Rev. E **54**, 3221 (1996).
[21]C. Yeung and Y. Oono, Europhys. Lett. **4**, 1061 (1987).
[22]A. Rodriguez, V. A. Malyshev, and F. Dominguez-Adame, J. Phys. A: Math. Gen. **33**, L161 (2000).
[23]A. Rodriguez, V. A. Malyshev, G. Sierra, M. A. Martin-Delgado, J. Rodriguez-Laguna, and F. Dominguez-Adame, Phys. Rev. Lett. **90**, 027404 (2003).
[24]A. V. Malyshev, V. A. Malyshev, and F. Dominguez-Adame, Phys. Rev. B **70**, 172202 (2004).
[25]F. A. B. F. de Moura, A. V. Malyshev, M. L. Lyra, V. A. Malyshev, and F. Dominguez-Adame, Phys. Rev. B **71**, 174203 (2005).
[26]F. Wegner, Z. Physik B **36**, 209 (1980).
[27]F. L. Metz, I. Neri, and D. Bollé, Phys. Rev. E **82**, 031135 (2010).
[28]F. Slanina, Eur. Phys. J. B **85**, 361 (2012).
[29]W. Kirsch and F. Martinelli, Commun. Math. Phys. **89**, 27 (1983).
[30]M. Ibanez Berganza and L. Leuzzi, arXiv:1211.3991v2.
[31]M. Janssen, Phys. Rep. **295**, 1 (1998).
[32]Y. Song, W. A. Atkinson, and R. Wortis, Phys. Rev. B **76**, 045105 (2007).
[33]E. N. Economou and M. H. Cohen, Phys. Rev. B **5**, 2931 (1972).
[34]Y. V. Fyodorov and A. D. Mirlin, Phys. Rev. Lett. **67**, 2049 (1991).
[35]J. Bauer, T.-M. Chang, and J. L. Skinner, Phys. Rev. B **42**, 8121 (1990).
[36]T.-M. Chang, J. Bauer, and J. L. Skinner, J. Chem. Phys. **93**, 8973 (1990).
[37]D. H. Dunlap, H.-L. Wu, and P. W. Phillips, Phys. Rev. Lett. **65**, 88 (1990).
[38]F. C. Lavarda, M. C. dos Santos, D. S. Galvão, and B. Laks, Phys. Rev. Lett. **73**, 1267 (1994).
[39]F. A. B. F. de Moura and M. L. Lyra, Phys. Rev. Lett. **81**, 3735 (1998).
[40]Mathematically, Eqs. (6) and (7) are equivalent to recursive computation of the Schur complement.